

Accurate prediction of defect properties in density functional supercell calculations

This content has been downloaded from IOPscience. Please scroll down to see the full text.

2009 Modelling Simul. Mater. Sci. Eng. 17 084002

(<http://iopscience.iop.org/0965-0393/17/8/084002>)

View [the table of contents for this issue](#), or go to the [journal homepage](#) for more

Download details:

IP Address: 202.120.224.18

This content was downloaded on 20/04/2017 at 16:42

Please note that [terms and conditions apply](#).

You may also be interested in:

[Issues in first-principles calculations for defects in semiconductors and oxides](#)

Risto M Nieminen

[Density functional theory calculations of defect energies using supercells](#)

C W M Castleton, A Höglund and S Mirbt

[First-principles determination of defect energy levels through hybrid density functionals and GW](#)

Wei Chen and Alfredo Pasquarello

[Point defects in ZnO: an approach from first principles](#)

Fumiyasu Oba, Minseok Choi, Atsushi Togo et al.

[Simple intrinsic defects in gallium arsenide](#)

Peter A Schultz and O Anatole von Lilienfeld

[A hybrid density functional view of native vacancies in gallium nitride](#)

Roland Gillen and John Robertson

[Geometry, electronic structure and thermodynamic stability of intrinsic point defects in indium oxide](#)

Péter Ágoston, Paul Erhart, Andreas Klein et al.

[Computational studies of conductivity in wide-band-gap semiconductors and oxides](#)

C G Van de Walle

[Theoretical studies of defect states in GaTe](#)

Zs Rak, S D Mahanti, Krishna C Mandal et al.

Accurate prediction of defect properties in density functional supercell calculations

Stephan Lany and Alex Zunger

National Renewable Energy Laboratory, Golden, CO 80401, USA

Received 8 July 2009, in final form 13 October 2009

Published 23 November 2009

Online at stacks.iop.org/MSMSE/17/084002

Abstract

The theoretical description of defects and impurities in semiconductors is largely based on density functional theory (DFT) employing supercell models. The literature discussion of uncertainties that limit the predictivity of this approach has focused mostly on two issues: (1) finite-size effects, in particular for charged defects; (2) the band-gap problem in local or semi-local DFT approximations. We here describe how finite-size effects (1) in the formation energy of charged defects can be accurately corrected in a simple way, i.e. by potential alignment in conjunction with a scaling of the Madelung-like screened first order correction term. The factor involved with this scaling depends only on the dielectric constant and the shape of the supercell, and quite accurately accounts for the full third order correction according to Makov and Payne. We further discuss in some detail the background and justification for this correction method, and also address the effect of the ionic screening on the magnitude of the image charge energy. In regard to (2) the band-gap problem, we discuss the merits of non-local external potentials that are added to the DFT Hamiltonian and allow for an empirical band-gap correction without significantly increasing the computational demand over that of standard DFT calculations. In combination with LDA + U , these potentials are further instrumental for the prediction of polaronic defects with localized holes in anion-p orbitals, such as the metal-site acceptors in wide-gap oxide semiconductors.

(Some figures in this article are in colour only in the electronic version)

1. Introduction

For the theoretical description of defects and impurities, the central quantity of interest is the defect formation energy ΔH_D , which determines, for example, the defect concentrations in equilibrium [1–5], and the thermodynamic transition energies between the different possible charge states of electrically active defects [6]. Notwithstanding the ground state formalism of density functional theory (DFT), one can also determine optical excitation or recombination

energies from ΔH_D , as long as the transitions occur as a result of the exchange of electrons with a distant reservoir, such as the band-edge states hosting the free carriers, or if the optically excited state is the lowest energy state of a given symmetry [7]. Thus, the formation enthalpy ΔH_D is the most decisive quantity for the functionality of semiconducting materials in regard to the presence and properties of defects or impurities. Within a supercell model, the formation energy is calculated as

$$\Delta H_{D,q}(E_F, \mu) = [E_{D,q} - E_H] + \sum_{\alpha} n_{\alpha} \mu_{\alpha} + q \cdot E_F, \quad (1)$$

where $E_{D,q}$ is the total energy of the supercell containing the defect in the charge state q and E_H is the respective supercell energy of the host without the defect. The chemical potentials μ_{α} describe the energy of the atomic reservoir of the atoms α removed ($n_{\alpha} = +1$) or added ($n_{\alpha} = -1$) to the host crystal when the defect is formed. For charged defects ($q \neq 0$), the Fermi energy E_F describes the energy of the reservoir for the electrons, which is typically considered to range between the valence band maximum (VBM) and the conduction band minimum (CBM), except for conditions of extremely high doping, e.g. in transparent conducting oxides [4], where E_F can reach a few tenths of an electronvolt into the conduction band.

For the accurate calculation of $\Delta H_{D,q}$ one needs to pay special attention to two different types of uncertainties, i.e. those that arise due to finite-size effects within supercell models, and those that arise due to inaccuracies in the underlying approximation for the energy functional. Regarding finite-size effects (1), it has been recognized that the average potentials of the charged defect calculation and that of the unperturbed host need to be aligned [3, 8], and that corrections are needed to account for the electrostatic interaction of the periodic images of the charged defects. Leslie and Gillian [9] suggested using the screened Madelung-energy of point charges compensated by a background to correct the image interaction. Makov and Payne [10] later extended this picture by introducing a third order term accounting for the interaction of the delocalized part of the defect-induced charge with the screened point-charge potential of the images. However, numerous applications over the past decade have drawn a mixed picture about the appropriateness of such corrections [11–24]. Only recently, were we able to demonstrate [25] by calculation of large supercells up to 1728 atoms that a very good convergence can be obtained when the third order image charge correction is combined with a potential alignment procedure, and when finite-size effects that are not related to the presence of a net charge are excluded or addressed separately. Note also that in a recent work of Freysoldt *et al* [26], very good convergence has been achieved as well with a method that does not utilize the expansion of Makov and Payne [10], but instead calculates the respective interaction energies from the calculated charge densities and the electrostatic potentials of the defect and of a reference (e.g., pure host) supercell.

In this work, we discuss in more detail than before the background and the justification for the potential alignment and the image charge corrections, and address the issue of electronic versus ionic screening for the image charge interaction.

Regarding the errors associated with the functional (2), a lot of attention has been paid to the ‘band-gap problem’ occurring in calculations of semiconductors and insulators based on the local density or generalized gradient approximation (LDA or GGA). In general, defect formation energies are affected by the band-gap problem in two ways. First, defect states may occur outside the band gap as resonances within the continuum of host states, whereas after opening of the band gap they should occur inside the gap. As a result of the incorrect placement of the defect level relative to the host band, electron-occupied defect states can incorrectly spill the electron into the conduction band [27], or hole defects can incorrectly spill the hole into the valence band. In this case, even the calculated charge density is incorrect

leading to an uncontrolled error in ΔH_D . Second, in the case of charged defects, $\Delta H_{D,q}$ depends linearly on the Fermi level (see equation (1)), which is bounded by the band-edge energies. When the band gap is changed, the range of formation energies between $E_F = E_{\text{VBM}}$ and $E_F = E_{\text{CBM}}$ changes accordingly. In order to cope with the band-gap problem for defect calculations, numerous methods and schemes of band-gap corrections for defect calculations have been proposed [6, 18, 22, 25, 28–34]. We also note that beyond the band-gap problem *per se*, the underlying approximation of the DFT functional may of course also affect the defect states directly, e.g. leading to a qualitatively wrong description of localized hole states in compound semiconductors [35–39]. Furthermore, the chemical potentials μ_α that enter the expression for the formation energy in equation (1) are bounded by the respective elemental phases of the atoms α . Here, the incomplete error cancellation between the total energies of the semiconductor compound and that of the elemental phases in general affects the defect formation energies. Improved bounds for the chemical potentials can be obtained through the optimized elemental reference energies of [40].

For the purpose of band-gap corrected defect calculation, much effort has recently been focused on post-LDA methods such as hybrid DFT [21, 24, 41–44], the related screened exchange (sX) method [45], GW [44, 46–48] or quantum Monte Carlo [49]. Common to these methods is that they are computationally much more demanding than standard DFT calculations. Also, hybrid DFT does not necessarily yield very accurate defect levels when the parameters are adjusted so as to match the experimental band gap [50]. Thus, there exists a desire for self-consistently band-gap corrected methods that are not significantly more expensive than standard LDA. For example, an empirical correction for the band gap can be achieved using parametrized potentials that are added to the DFT Hamiltonian [51, 52]. A similar band-gap opening effect is obtained by the LDA + U method, when applied not only to cation-d states, but also to cation-s or anion-s states [23, 25, 33, 53], or by an atomic-orbital based variant [32, 54] of the self-interaction correction (SIC) [55]. In order to achieve a flexible means for empirical adjustment of the band structure, we recently [27] introduced non-local external potentials (NLEP) whose implementation is similar to the respective LDA + U potentials, but which do not depend on the orbital occupation. Here, we describe more details of this method and discuss possible extensions.

2. Finite-size effects due to charged defects

2.1. The need for potential alignment

When periodic boundary conditions are applied, the total energy of a system with a net charge is ill-defined due to the divergence of the electrostatic potential. Depending on the particular implementation of the energy expression, e.g. that of [56] for pseudopotential methods, the calculated total energy E follows Janak's theorem

$$\frac{dE(n_i)}{dn_i} = e_i, \quad (2)$$

upon variation of the occupation number n_i of the highest occupied state i with the eigenvalue e_i . In particular, the energy of a hole at the VBM in a unit of a semiconductor host (H) with N electrons is then obtained as

$$\lim_{N \rightarrow \infty} [E_H(N) - E_H(N - 1)] = e_{\text{VBM}}, \quad (3)$$

i.e. the hole energy equals the eigenvalue of the VBM in the limit of a infinite system (in practice, this result can be calculated within a small unit cell and fractional charges [34]). Thus, the eigenvalue e_{VBM} can be used as the reference energy for the electron reservoir in equation (1),

i.e. $E_F = e_{\text{VBM}} + \Delta E_F$, where ΔE_F denotes the position of the Fermi level within the semiconductor band gap ($0 < \Delta E_F < E_g$).

Since the (otherwise divergent) average electrostatic (el) potential within the cell is conventionally set to zero within the pseudopotential momentum-space formalism [56], i.e. $V_{\text{el}}(\mathbf{G} = 0) = 0$, the eigenvalues are defined only up to an undetermined constant. Whereas the total energy of a charge-neutral system is a well-defined quantity [56], the ‘charged energies’ depend on the same undetermined constant as the eigenvalues, which can be seen from equations (2) and (3). While the omission of the $\mathbf{G} = 0$ term of the Fourier expansion is often described as in effect introducing a compensating background charge, it is important to note that the charge compensation occurs only in the *potential*, but a background *charge density* is usually not explicitly introduced into the calculation. Note that if a compensating charge density were introduced, the resulting overall charge-neutral system should have a well-defined total energy and not depend on the undetermined constant [25]. While the energy of the ‘charged cell + background density’ in principle can be calculated, it is usually not desirable to have the interaction energy of the background with all N electrons and Z ionic charges included in the total energy.

In order to obtain a physically meaningful formation energy $\Delta H_{\text{D},q}$ without explicitly introducing the interaction with a background density, one can use the total energy calculated with the usual energy expression [56] for which equation (2) holds, and then correct for the undetermined offset by ensuring that the undetermined constants in $E_{\text{D},q}$ and in e_{VBM} are consistent. That is, one needs to restore the relative positions of the average potential in the calculations of the defect (affecting $E_{\text{D},q}$) and the pure host (affecting e_{VBM}). This is achieved by means of a ‘potential alignment’ (pa) correction that is added to the formation energy:

$$\Delta E_{\text{pa}}(\text{D}, q) = q \cdot \Delta V_{\text{pa}}, \quad (4)$$

where ΔV_{pa} is the potential alignment between the defect and the host calculation, respectively. For practical calculations we use as reference potentials the atomic-site electrostatic potentials $V_{\text{D}}^{\alpha 1}$, serving as ‘potential markers’. The potential alignment $\Delta V_{\text{pa}} = \overline{(V_{\text{D}}^{\alpha} - V_{\text{H}}^{\alpha})}$ is then determined as the average difference between $V_{\text{D},q}^{\alpha}$ in the defect supercell and the respective V_{H}^{α} in the pure host. The immediate neighbors of the defect are excluded from averaging, since their atomic potentials can be affected by the chemical interaction with the defect. For the case of the As vacancy V_{As}^{3+} in GaAs, which we used in [25] as a test case to study finite-size effects, figure 1 shows the potential difference $V_{\text{D},q}^{\alpha}(r) - V_{\text{H}}^{\alpha}(r)$ as a function of the distance r from the defect. If the supercell is large enough (e.g., 1000 atoms in figure 1(a)), the atomic-site potentials clearly reflect the shape of the long-ranged screened electrostatic potential due to the charged defect (and its images).

2.2. Correction of image charge interactions

The leading (first order) correction term for the electrostatic interaction energy between the images (i) of charged supercells is the screened Madelung-like lattice energy of point charges [9],

$$\Delta E_{\text{i}}^1 = \frac{q^2 \alpha_{\text{M}}}{2\epsilon L}, \quad (5)$$

where $L = \Omega^{-1/3}$ is the linear supercell dimension (supercell volume Ω), ϵ is the dielectric constant and α_{M} is the appropriate Madelung constant for the respective supercell geometry.

¹ The atomic-site potentials $V_{\text{D},q}^{\alpha}$ are determined as the average electrostatic potential in a small sphere around an atom [57].

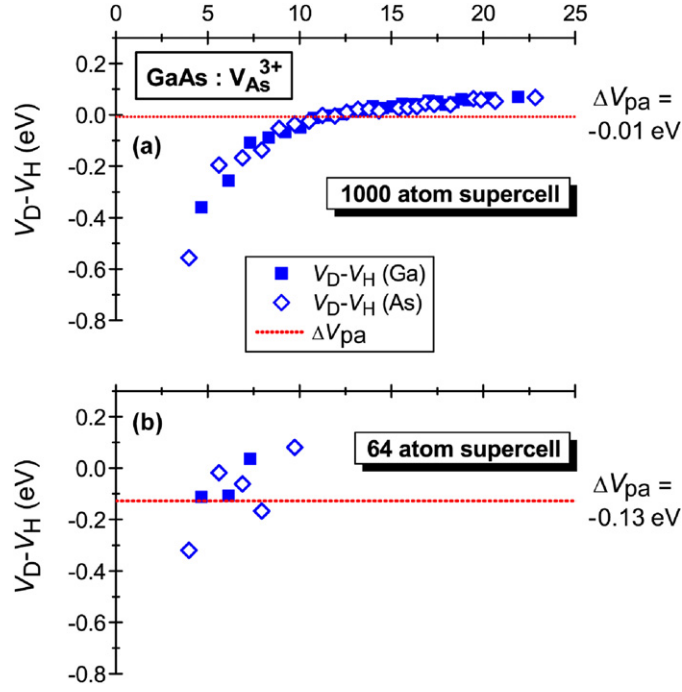


Figure 1. The difference in the atomic-site potentials V_{Ga} and V_{As} between a supercell containing a vacancy V_{As}^{3+} and the defect-free host, shown for 1000 atom supercell (a) and a 64 atom supercell (b).

Addressing primarily the case of molecules in vacuum ($\epsilon = 1$), Makov and Payne derived an expression for a third order correction term by decomposing the total charge into a point charge plus an extended (e), net neutral density $\rho_e(\mathbf{r})$. In this case, the energy correction due to the energy of $\rho_e(\mathbf{r})$ in the potential of the point-charge images (quadrupole–monopole interaction) is

$$\Delta E_i^3 = \frac{2\pi q Q_r}{3\epsilon L^3}, \quad (6)$$

where

$$Q_r = \int_{\Omega} d^3r \rho_e(\mathbf{r}) r^2 \quad (7)$$

is the second radial moment of the extended charge density. Since, for the case of molecules in vacuum, $\rho_e(\mathbf{r})$ is confined within the supercell, the interaction energy between $\rho_e(\mathbf{r})$ and its images (without the point-charge contribution) scales as $O(L^{-5})$ and is neglected.

When translating these results for molecules in vacuum to the case of defects in solids ($\epsilon \gg 1$), the defect-induced electronic charge density, $\Delta\rho_D(\mathbf{r}) = \rho_D(\mathbf{r}) - \rho_H(\mathbf{r})$ (ρ_D = charge density in the defect supercell; ρ_H = density in the unperturbed host supercell) takes the place of the extended density $\rho_e(\mathbf{r})$ in equation (7), and the total energy correction $\Delta E_i = \Delta E_i^1 + \Delta E_i^3$ is calculated as the sum of the first and third order terms, equations (5) and (6), respectively. In [25], we demonstrated for a number of defects in GaAs that the image charge correction calculated in this way, in conjunction with the potential alignment (see above), provides for excellent convergence of the $\Delta H_{D,q}$ with respect to the supercell size, being well converged already for typical cell sizes of 64 atoms. The results for the triply charged As vacancy V_{As}^{3+} in the zinc-blende lattice of GaAs are shown in figure 2, where the atomic relaxation

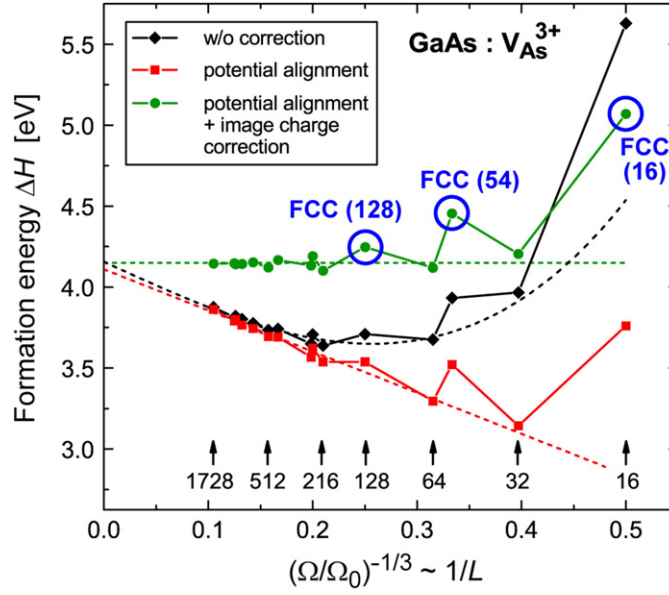


Figure 2. The formation energy ΔH of the V_{As}^{3+} defect in GaAs ($E_F = E_V$, As-rich conditions) as a function of the inverse linear supercell dimension $1/L = \Omega^{-1/3}$ (Ω = supercell volume, Ω_0 = volume of the 2 atom GaAs unit cell). (Modified from [25].)

was constrained so as to exclude finite-size effects originating from elastic energies [25]. Less satisfying convergence was observed only for the face-centered cubic (FCC) supercell symmetries (e.g., 16, 54, 128 atoms), which was attributed to the fact that in these geometries, the defects are aligned along the (1 1 0) zig-zag chains, which promote strong direct defect–defect interactions. Consequently, these supercells are generally not recommended for defect calculations.

While the image charge correction according to equations (5)–(7) proved very successful, there exist a few conceptional issues regarding the application in semiconductors, which we address now. First, in their original paper, Makov and Payne surmised that the density entering the integration of Q_r (see equation (7)) should contain only that part of $\Delta\rho_D(r)$ that does not arise from electronic screening. However, we found in [25] that Q_r is actually dominated by contribution to $\Delta\rho_D(r)$ arising from the screening response upon introduction of a charged defect into the semiconductor host. Excluding this part would greatly reduce the magnitude of ΔE_i^3 and significantly worsen the convergence behavior. Second, since the defect density $\Delta\rho_D(r)$ is largely due to the screening response of the host, it is not confined within the supercell, but extends toward the space between the images. Thus, superficially, it seems unjustified to neglect the interaction energy between the extended densities $\Delta\rho_D(r)$, i.e. the quadrupole–quadrupole interaction as was done in the case of confined density $\rho_e(r)$ for molecules in vacuum.

In order to resolve these apparent conceptional conflicts, we now discuss in more detail the image charge interactions in the presence of a dielectric medium: The total (electron + ion) charge density in the defect supercell, can be written as $\rho_H^{\text{tot}}(r) + \Delta\rho_p(r) + \Delta\rho_D(r)$, where $\Delta\rho_p(r)$ is the point-charge-like contribution due to the ionic substitution, which is assumed here to include also a compensating background. The image charge correction is the difference between the electrostatic interaction energy of the supercell with an environment (env) of unperturbed host supercells minus the interaction energy of the supercell with an environment

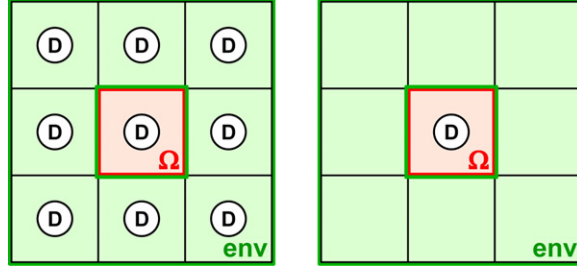


Figure 3. Schematic illustration of a defect supercell (Ω) in an environment (env) of periodic images (left) or in an environment of host cells (right).

of identical defect supercells (see figure 3):

$$\Delta E_i = - \int_{\Omega} d\mathbf{r}^3 (\rho_H^{\text{tot}}(\mathbf{r}) + \Delta\rho_p(\mathbf{r}) + \Delta\rho_D(\mathbf{r})) \int_{\text{env}} d\mathbf{r}'^3 \frac{\Delta\rho_p(\mathbf{r}') + \Delta\rho_D(\mathbf{r}')}{|\mathbf{r} - \mathbf{r}'|}. \quad (8)$$

Under the approximation that the supercell is large enough so that each unit cell of the pure host appears as a neutral object on the scale of the supercell (despite being modulated within a unit cell), we can neglect the interaction energy of $\rho_H^{\text{tot}}(\mathbf{r})$ with the total defect-induced density $[\Delta\rho_p(\mathbf{r}') + \Delta\rho_D(\mathbf{r}')] in the image supercells. Thus, excluding the term involving $\rho_H^{\text{tot}}(\mathbf{r})$, we can express equation (8) as the sum of interactions between the subsystems ρ_p and ρ_D :$

$$\Delta E_i = -(E_{p,p} + E_{p,D} + E_{D,D}). \quad (9)$$

At this point we observe that (i) so far no screening has been invoked and (ii) equation (9) contains the quadrupole–quadrupole term $E_{D,D}$ which cannot be neglected because the density $\Delta\rho_D(\mathbf{r})$ is not confined within the supercell. However, considering that $\Delta\rho_D(\mathbf{r})$ essentially reflects the screening response of the host upon introduction of the charged defect [25], we can interpret the integral over the volume ‘env’ in equation (8) as the *screened* potential $V_{\text{scr}}^{\text{env}}(\mathbf{r})$ created by the point charges in the supercell images and their compensating background:

$$\Delta E_i = - \int_{\Omega} d\mathbf{r}^3 (\Delta\rho_p(\mathbf{r}) + \Delta\rho_D(\mathbf{r})) V_{\text{scr}}^{\text{env}}(\mathbf{r}). \quad (10)$$

The interaction energy between screened point-charge potential $V_{\text{scr}}^{\text{env}}(\mathbf{r})$ with $\Delta\rho_p(\mathbf{r})$ and with $\Delta\rho_D(\mathbf{r})$ corresponds to the first and third order terms, equations (5) and (6), respectively, when the screening response of the host is *included* in $\Delta\rho_D(\mathbf{r})$. Thus, comparing equation (10) with equation (9), we see that after electronic screening is accounted for, the quadrupole–quadrupole does not enter anymore. It is therefore justified to truncate the expansion beyond the third order term despite the fact that the delocalized part of the defect-induced charge extends up to the border of the supercell.

Regarding the role of the compensating background, we again note that the total energy does not include the (undesired) electrostatic interaction of the background with the full electron+ion system ($\sim N$ charges), since the background is not explicitly included in the charge density of the supercell (see above). Rather, as seen from equation (8) after dropping the term with ρ_H^{tot} , the only interaction energy involving the background is that between the background and the defect-induced charge ($\sim q$ charges) in the surrounding supercells. This artificial interaction energy is corrected for by the image charge interaction according to equations (5) and (6).

Table 1. The factors c_{sh} for the simplified expression, equation (11) of the image charge correction, given for the supercell geometries SC, FCC, BCC, HCP and a $3 \times 3 \times 2$ multiple of the ideal HCP cell.

Supercell geometry	c_{sh}
SC	−0.369
FCC	−0.343
BCC	−0.342
HCP	−0.478
HCP ($3 \times 3 \times 2$)	−0.365

2.3. Simplified expression for the image charge correction

The observation that the delocalized part of the defect-induced density, $\Delta\rho_{\text{D}}(\mathbf{r})$, is dominated by the screening response of the host has the important consequence that the second radial moment Q_r entering the third order correction term, equation (6), is proportional to q and to L^2 , such that the ΔE_{i}^3 scales effectively as $\propto q^2/L$ instead of the nominal $\propto q/L^3$ scaling implied by equation (6). Thus, the full first plus third order image charge correction ΔE_{i} can be accounted for by a simple scaling of the first order Madelung-like term [25]. We now use this finding to give a simplified expression for ΔE_{i} . Considering that the electronic charge that accumulates close to the defect due to dielectric screening is drawn more or less homogeneously from the entire supercell [25], the defect-induced charge density is approximately $\Delta\rho_{\text{D}}(r > l_{\text{scr}}) \approx \frac{1}{\Omega}q(1 - \varepsilon^{-1})$ for distances r from the defect that are larger than the screening length l_{scr} , i.e. at those distances that dominate the integration of Q_r (due to the r^2 factor in the integrand of equation (7)). Thus, we can express the full image charge correction approximately by the first order correction ΔE_{i}^1 , equation (5), times a factor that depends only on the dielectric constant ε and on the shape (sh) of the supercell:

$$\Delta E_{\text{i}} = [1 + c_{\text{sh}}(1 - \varepsilon^{-1})]\Delta E_{\text{i}}^1. \quad (11)$$

The shape factors c_{sh} can easily be calculated using equations (5)–(7), by performing the integration in equation (7) over the Wigner–Seitz cell with a constant charge density. In table 1, we give the numerical values of c_{sh} for simple cubic (SC), face-centered cubic (FCC), body-centered cubic (BCC), hexagonal close packed (HCP) cells and for a $3 \times 3 \times 2$ HCP supercell. For the cubic supercells, the values of c_{sh} are close to $-1/3$. The ideal HCP geometry has a larger c_{sh} (absolute value) which is due to its rather anisotropic shape (aspect ratio). The more isotropic $3 \times 3 \times 2$ supercell, as used below for defect calculations in wurtzite ZnO, however, has a value of c_{sh} similar to the cubic geometries. Thus, we see that equation (11) reduces to $\Delta E_{\text{i}} \approx 2/3 \Delta E_{\text{i}}^1$ if two conditions are fulfilled, i.e. (i) the dielectric constant is sufficiently large ($\varepsilon \gg 1$) and (ii) the supercell is approximately isotropic. This explains the earlier empirical observation that $\Delta E_{\text{i}} \approx 2/3 \Delta E_{\text{i}}^1$ when the third order term was calculated from the actual defect-induced density $\Delta\rho_{\text{D}}$ determined from the self-consistent defect calculation [32].

2.4. The role of ionic screening

In order to examine the scaling behavior of the electrostatic interactions, some previous works [20, 25, 26] have used a constrained relaxation (e.g., only nearest neighbors [25]), so as to eliminate the effect of elastic energies from the finite-size scaling. In this situation, the interaction between the charged defect and its images is only electronically screened, i.e. one would use the static electronic (e) dielectric constant $\varepsilon = \varepsilon_{\text{e}}$ to determine the image charge correction in equations (5), (6) and (11). In practical applications, however, one is generally interested in the defect properties including full relaxation. In this situation, ionic screening

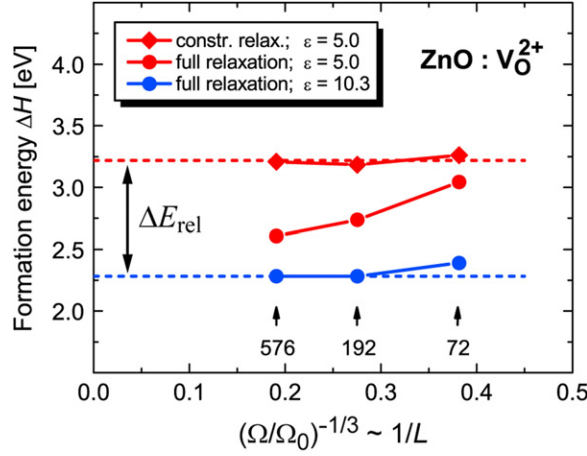


Figure 4. Finite-size scaling of ΔH for the V_O^{2+} defect in ZnO ($E_F = E_V$, O-rich) in GGA, calculated with constrained atomic relaxation (diamonds) and with full relaxation (circles). The image charge correction is determined using $\epsilon_\infty = 5.0$ or $\epsilon_0 = 10.3$.

also contributes to the screening of the image charge energy, so that the total (electronic+ionic), i.e. the low-frequency dielectric constant $\epsilon = \epsilon_0$ is appropriate, proposed that the supercell dimension is sufficiently large compared with the effective screening length.

Using 72, 192 and 576 atom supercells of the wurtzite lattice, we show in figure 4 the finite-size scaling of V_O^{2+} in ZnO, where there exists a larger difference between ϵ_0 and ϵ_e than, e.g., in GaAs. We determine here $\epsilon_e = 5.0$ from a calculation with a periodically modulated external field, in agreement with previous calculations based on density functional perturbation theory [58, 59], and we use $\epsilon_0 = 10.3$ from [58]. In a calculation with constrained atomic relaxation, as determined for the nearest and next nearest neighbor shells in the 72 atom cell, we find that finite size effects are very well eliminated if we apply the image charge correction according to equation (11) (with respective factors c_{sh} for the actual cell geometries), and if we use the electronic dielectric constant $\epsilon = \epsilon_e$ (figure 4). Similarly, converged formation energies for the fully relaxed situation are obtained, if we instead use the low-frequency dielectric constant $\epsilon = \epsilon_0$. The difference, $\Delta E_{rel} = -0.94$ eV, accounts for the (elastic) relaxation energy when atomic relaxation beyond the second shell is taken into account. For illustration, we further show in figure 4 the formation energies for the fully relaxed supercell, but using ϵ_e (only electronic screening). In this case, considerable finite-size effects remain, and we emphasize that the apparent relaxation energy, obtained without considering the reduction of the image charge energy due to ionic screening, is considerably smaller than the true relaxation energy, in particular for small cells, e.g. the apparent relaxation energy is only $\Delta E_{rel} = -0.18$ eV in the 72 atom cell (see figure 4). Thus, in general, it is important to account for the ionic contribution to the screening when determining the magnitude of the image charge correction.

3. Correction of the band-gap problem

3.1. The aim of self-consistent band-gap correction

Ever since the first predictions of defects in semiconductors within the LDA [6, 60], the ‘band-gap problem’ pervasively troubled the literature on the theoretical prediction of defect properties, and a range of band-gap correction methods emerged, many of which apply energy

corrections to the defect formation energy but still rely on the self-consistent LDA defect calculation [6, 18, 22, 25]. In many cases, however, the very small band gap leads to a spurious hybridization between the defect states and the host bands, leading to a qualitatively wrong description of the defect state [27]. In these cases, the gap correction within the self-consistent calculation is indispensable. In order to correct the band structure of the semiconductor host within the self-consistent calculation, Christensen [51] introduced additional potentials, which were empirically adjusted to match the experimental band structure. In a similar spirit, the LDA + U method [61–64], which is typically used to improve the LDA description of cation-d states, was applied for band-gap corrected defect calculations, where it acts to open the band gap when using *negative* values for U on anion-s states [33, 53], or very large positive values for U on cation-s states [23, 25]. Self-consistently band-gap corrected defect calculations have also been performed [65] on the basis of SIC [55] in a simplified implementation [32, 54] that, similar to LDA + U , employs atomic projections. Recently, hybrid-DFT calculations which mitigate the band-gap problem by a mixing of the density functional and Hartree–Fock exchanges became quite popular for defect calculations [21, 24, 41–45], although they are computationally still much more demanding than standard DFT calculations. Based on perturbation theory arguments, Perdew *et al* [66] suggested a parameter of 25% for the uniform mixing of the exact exchange for typical molecules, which, by extension, is also often preferred for solids. On the other hand, in practical applications of hybrid DFT to semiconductors or insulators, the mixing parameter is often also empirically chosen to match the experimental band gap [24, 67]. The uncertainties arising from the question how to mix the exact and the GGA exchange are avoided in GW, which, however, for the purpose of defect calculations is so far only feasible for determining the quasi-particle energies [44, 46], but not for self-consistent total-energy calculation.

3.2. Empirical NLEP

Given that fully parameter-free and accurate post-LDA methods such as GW or quantum Monte Carlo [49] remain very demanding for defect systems which typically require a system size on the order of 100 atoms, an alternative route is to devise computationally effective parametrized functionals that can be employed for very large systems or for a very large number of calculations, once the parameters have been fitted to high-accuracy reference calculations, or to experiment. In this vein, non-self-consistent (semi-) empirical pseudopotentials [68] can be applied to large scale problems such as quantum dots and nanostructures without the band gap problem [69]. In order to achieve a self-consistent band-gap correction that can be applied to defects, including different charge states and atomic relaxation, we recently introduced NLEP, which are parameterized in the atom type α and the angular momentum l [27]. The implementation of these potentials into the projector-augmented wave (PAW) method [70, 71] employs the PAW projectors p_i and the all electron partial waves ϕ_i^{AE} which depend on an index i that comprises the atomic site α , the angular momentum numbers l, m and an index k for the reference energy used to determine the partial waves ϕ_i^{AE} [71]. Thus, the functional form of the NLEP potential is analogous to the LDA + U potential [72]:

$$\hat{V}_{\alpha,l}^{\text{NLEP}} = \sum_{i,j} |p_i\rangle \langle \phi_i^{\text{AE}} | V_{\alpha,l}^{\text{NLEP}} | \phi_j^{\text{AE}} \rangle \langle p_j|, \quad (12)$$

but contrary to LDA + U , the potential strength parameters $V_{\alpha,l}^{\text{NLEP}}$ are free parameters that do not depend on the orbital occupancies. In equation (12), the sum runs only over those i and j that contain the atom type α and angular momentum l for the specified NLEP potential.

A further difference between NLEP and LDA+ U is that the total-energy contribution due to the NLEP potential is not derived from a model for the electron–electron interaction. Whereas LDA + U is derived from a (screened) Hartree–Fock-like interaction [61, 62], the NLEP are treated as simple external potentials. Since, the interaction energy between the electrons and an external potential is contained in the sum of occupied eigenvalues, no additional terms for the total energy are needed. For example, we used in [27, 73] the NLEP method to predict the defect levels of transition metals in ZnO and In₂O₃, where the main contribution to the band-gap correction comes from the repulsive NLEP potential for cation-s states. According to equation (12), e.g. the NLEP potential $V_{\text{Zn-s}}^{\text{NLEP}}$ leads to an energy contribution $E_{\text{Zn-s}}^{\text{NLEP}}$ in the sum over the occupied eigenvalues e_n of the corresponding Kohn–Sham orbitals ψ_n :

$$E_{\text{Zn-s}}^{\text{NLEP}} = V_{\text{Zn-s}}^{\text{NLEP}} \sum_{n=\text{occ.}} \sum_{i,j} \langle \psi_n | p_i \rangle \langle \phi_i^{\text{AE}} | \phi_j^{\text{AE}} \rangle \langle p_j | \psi_n \rangle, \quad (13)$$

which equals simply the potential strength times the Zn-s partial charge $n_{\text{Zn-s}}$:

$$E_{\text{Zn-s}}^{\text{NLEP}} = V_{\text{Zn-s}}^{\text{NLEP}} n_{\text{Zn-s}}. \quad (14)$$

In order to achieve an optimal overall description of the band structure and structural properties, we used in [27, 73] not only NLEP potentials for Zn-s, but also for Zn-p and for O-s/p. A drawback of the NLEP method is that the static NLEP potentials act to change the charge density in an unphysical way. For example, while the repulsive $V_{\text{Zn-s}}^{\text{NLEP}}$ potential increases the band gap in ZnO by shifting the Zn-s-like conduction band states to a higher energy, it also acts to reduce the Zn-s partial charge that exists due to the partially covalent character of the Zn–O bonds. Thus, the band-gap correction by NLEP renders ZnO more ionic than in LDA or GGA, which is probably unphysical. While we confirmed for the cases studied in [27, 73] by variation of the NLEP parameters that the reduction of the Zn-s partial charge does not significantly affect the predicted defect levels of the transition metals, one would in general like to achieve the band-gap correction without adverse effects on the charge density. Possible extensions of the NLEP potentials, e.g. by including the dependence on the energy parameter k in the NLEP parameters, $V_{\alpha,l,k}^{\text{NLEP}}$, are expected to accomplish this [74].

Apart from the empirical band-gap correction, the NLEP potentials proved useful for the prediction of polaronic hole states in oxides [37, 39], such as the acceptor states introduced by Li_{Zn} or the cation vacancy V_{Zn} in ZnO, and the metal-site acceptors in other oxides such as In₂O₃ and SnO₂. While it is generally known that such localized hole states are incorrectly described in standard DFT functionals as rather delocalized states that spread over all oxygen ligands [35–39], the quantitative prediction of the acceptor states remains challenging. For example, the LDA + U potential, e.g. in the form of [64],

$$V_{m,\sigma}^U = U^{\text{eff}} (\frac{1}{2} - n_{m,\sigma}), \quad (15)$$

qualitatively restores the correct localization of the acceptor state of Al_{Si} in SiO₂ on just one O ligand when it is applied on O-p states [37]. However, it simultaneously distorts the underlying host band structure in a rather uncontrolled way, because the O-p partial charge $n_{\text{O-p}}$ depends sensitively on the integration radius used for LDA + U [38]. In order to avoid such ambiguities, we introduced in [38] a hole-state potential of the form

$$V_{\text{hs}} = \lambda_{\text{hs}} (1 - n_{m,\sigma} / n_{\text{host}}), \quad (16)$$

where n_{host} is the O-p partial charge of the unperturbed (defect-free) oxide host and λ_{hs} is a potential strength parameter. The specific form, equation (16), of the hole-state potential can be easily constructed by the combination of the NLEP and LDA + U potentials, using

$$U_{\text{O-p}}^{\text{eff}} = \lambda_{\text{hs}} / n_{\text{host}} \quad (17)$$

and

$$V_{\text{O-p}}^{\text{NLEP}} = \lambda_{\text{hs}}(1 - 0.5/n_{\text{host}}), \quad (18)$$

and it ensures that the underlying host band structure is not affected [38], in contrast to LDA + U . Further, the strength parameter λ_{hs} is determined by the fundamental requirement that the energy must be a piecewise linear function of the (fractional) number of electrons between integers [75–77]. Using this condition, the correction of the localized acceptor state (without band-gap correction) and the restoration of the correct splitting between occupied and unoccupied anion-p sublevels can be achieved fully non-empirically. Applying the hole-state correction in [35] to the metal-site acceptors in ZnO, In₂O₃ and SnO₂, we obtained much deeper acceptor levels than in standard LDA or GGA calculations, which curbs the expectations to achieve p-type doping by acceptor-like point defects in wide-gap oxide semiconductors. Studying the behavior of Zn vacancies in the series of Zn chalcogenides (ZnO, ZnS, ZnSe, ZnTe), we further demonstrated in [39] that the metallic-type band structure predicted in GGA for the host + vacancy system changes into an insulating-type akin to the situation in a Mott insulator, when the correct linear behavior of the energy as a function of the electron number is restored. Thus, quite unexpectedly, electronic correlation effects beyond LDA or GGA that cause such a transition from metallic to insulating behavior exist not only in anion-p shells of first row elements, such as oxygen, but also in much heavier anions such as Te. The qualitative change of the electronic structure of the vacancy defects has important consequences for the so-called d⁰ magnetism [78]. Corroborating the conclusions of Droghetti *et al* [79] based SIC, we found in [39] that the magnetic interaction between V_{Zn} vacancies is impeded when the localization of the holes is correctly described.

4. Conclusions

Finite-size effects due to charged defects in supercell calculations can be corrected by considering potential alignment and image charge corrections simultaneously. The expansion up to third order in the inverse linear supercell dimension, as suggested by Makov and Payne, provides a very accurate correction of the image charge energy if the full defect-induced density, including the contribution from dielectric screening, is considered for the calculation of the third order term. We further provided a justification for the truncation of the expansion after the third order term, despite the fact that the defect-induced density is not confined within the supercell. Based on the observation that the defect-induced density is actually dominated by the screening response of the host, we suggest a simple but accurate approximation of the full third order image charge correction, being expressed as the respective first order term times a factor that depends only on the shape of the supercell and the dielectric constant. We further demonstrated that the low-frequency dielectric constant determines the magnitude of the image charge correction if atoms within the entire supercell are allowed to relax, whereas the ion-clamped (electronic-only) dielectric constant is more appropriate if the atomic relaxation is restricted to a small volume around the defect.

With respect to the band-gap problem, we highlighted the desire for self-consistently band-gap corrected methods whose demand in computational resources does not significantly exceed that of standard DFT calculations. For this purpose, we described the addition of the NLEP to the DFT Hamiltonian, which carries the prospect of combining the benefits of empirical pseudopotentials and self-consistent DFT calculations. Apart from the application for band-gap correction, we have used these NLEP potentials also in combination with LDA+ U to define a ‘hole-state potential’ for polaronic, localized anion-p holes which are otherwise incorrectly described in standard DFT functionals. The correct description of the localization

of the anion-p hole and of the energy splitting between occupied and unoccupied sublevels has quite important ramifications for acceptor doping of wide-gap oxide semiconductors and for the prospects of d^0 magnetism.

Acknowledgments

This work was funded by the US Department of Energy, Office of Energy Efficiency and Renewable Energy, under Contract No DE-AC36-08GO28308 to NREL.

References

- [1] Kröger F A 1974 *The Chemistry of Imperfect Crystals* (Amsterdam: North-Holland)
- [2] Zhang S B and Northrup J E 1991 *Phys. Rev. Lett.* **67** 2339
- [3] Laks D B, van de Walle C G, Neumark G F, Blöchl P E and Pantelides S T 1992 *Phys. Rev. B* **45** 10965
- [4] Lany S and Zunger A 2007 *Phys. Rev. Lett.* **98** 045501
- [5] Lany S, Osorio-Guillén J and Zunger A 2007 *Phys. Rev. B* **75** 241203
- [6] Baraff G A and Schlüter M 1985 *Phys. Rev. Lett.* **55** 1327
- [7] Dabrowski J and Scheffler M 1989 *Phys. Rev. B* **40** 10391
- [8] Mattila T and Zunger A 1998 *Phys. Rev. B* **58** 1367
- [9] Leslie M and Gillian M J 1985 *J. Phys. C: Solid State Phys.* **18** 973
- [10] Makov G and Payne M C 1995 *Phys. Rev. B* **51** 4014
- [11] Schultz P A 2000 *Phys. Rev. Lett.* **84** 1942
- [12] Lento J, Mozos J-L and Nieminen R M 2002 *J. Phys.: Condens. Matter* **14** 2637
- [13] Gerstmann U, Deák P, Ruráli R, Aradi B, Frauenheim T and Overhof H 2003 *Physica B* **340–342** 190
- [14] Segev D and Wei S-H 2003 *Phys. Rev. Lett.* **91** 126406
- [15] Limpijumngong S, Zhang S B, Wei S-H and Park C H 2004 *Phys. Rev. Lett.* **92** 155504
- [16] van de Walle C G and Neugebauer J 2004 *J. Appl. Phys.* **95** 3851
- [17] Shim J, Lee E-K, Lee Y J and Nieminen R M 2005 *Phys. Rev. B* **71** 035206
- [18] Schultz P A 2006 *Phys. Rev. Lett.* **96** 246401
- [19] Castleton C W M, Höglund A and Mirbt S 2006 *Phys. Rev. B* **73** 035215
- [20] Wright A F and Modine N A 2006 *Phys. Rev. B* **74** 235209
- [21] Gali A, Hornos T, Son N T, Janzén E and Choyke W J 2007 *Phys. Rev. B* **75** 045211
- [22] Janotti A and van de Walle C G 2007 *Phys. Rev. B* **76** 165202
- [23] Paudel T R and Lambrecht W R L 2008 *Phys. Rev. B* **77** 205202
- [24] Oba F, Togo A, Tanaka I, Paier J and Kresse G 2008 *Phys. Rev. B* **77** 245202
- [25] Lany S and Zunger A 2008 *Phys. Rev. B* **78** 235104
- [26] Freysoldt C, Neugebauer J and van de Walle C G 2009 *Phys. Rev. Lett.* **102** 016402
- [27] Lany S, Raebiger H and Zunger A 2008 *Phys. Rev. B* **77** 241201
- [28] Svane A and Gunnarsson O 1990 *Phys. Rev. Lett.* **65** 1148
- [29] Zhang S B, Wei S-H and Zunger A 2000 *Phys. Rev. Lett.* **84** 1232
- [30] Stampfl C, van de Walle C G, Vogel D, Krüger P and Pollmann J 2000 *Phys. Rev. B* **61** R7846
- [31] Zhang S B, Wei S-H and Zunger A 2001 *Phys. Rev. B* **63** 075205
- [32] Filippetti A and Spaldin N A 2003 *Phys. Rev. B* **67** 125109
- [33] Persson C and Zunger A 2005 *Appl. Phys. Lett.* **87** 211904
- [34] Persson C, Zhao Y J, Lany S and Zunger A 2005 *Phys. Rev. B* **72** 035211
- [35] Pacchioni G, Frigoli F, Ricci D and Weil J A 2000 *Phys. Rev. B* **63** 054102
- [36] Lægsgaard J and Stokbro K 2001 *Phys. Rev. Lett.* **86** 2834
- [37] Nolan M and Watson G W 2006 *J. Chem. Phys.* **125** 144701
- [38] Lany S and Zunger A 2009 *Phys. Rev. B* **80** 085202
- [39] Chan J A, Lany S and Zunger A 2009 *Phys. Rev. Lett.* **103** 016404
- [40] Lany S 2008 *Phys. Rev. B* **78** 245207
- [41] To J, Sokol A A, French S A, Kaltsoyannis N and Catlow C R A 2005 *J. Chem. Phys.* **122** 144704
- [42] Patterson C H 2006 *Phys. Rev. B* **74** 144432
- [43] Sokol A A, French S A, Bromley S T, Catlow C R A, van Dam H J J and Sherwood P 2007 *Faraday Discuss.* **134** 267
- [44] Stroppa A and Kresse G 2009 *Phys. Rev. B* **79** 201201

- [45] Xiong K, Robertson J and Clark S J 2006 *J. Appl. Phys.* **99** 044105
- [46] Weber J R, Janotti A, Rinke P and Van de Walle C G 2007 *Appl. Phys. Lett.* **91** 142101
- [47] Ma Y and Rohlfing M 2008 *Phys. Rev. B* **77** 115118
- [48] Bockstedte M, Marini A, Gali A, Pankratov O and Rubio A 2009 *Mater. Sci. Forum* **600–603** 285
- [49] Batista E R, Heyd J, Hennig R G, Uberuaga B P, Martin R L, Scuseria G E, Umrigar C J and Wilkins J W 2006 *Phys. Rev. B* **74** 121102
- [50] Lany S and Zunger A, unpublished
- [51] Christensen N E 1984 *Phys. Rev. B* **30** 5753
- [52] Wei S H and Zunger A 1993 *Phys. Rev. B* **48** 6111
- [53] Walsh A, da Silva J L F and Wei S H 2008 *Phys. Rev. Lett.* **100** 256401
- [54] Pemmaraju C D, Archer T, Sánchez-Portal D and Sanvito S 2007 *Phys. Rev. B* **75** 045101
- [55] Perdew J P and Zunger A 1981 *Phys. Rev. B* **23** 5048
- [56] Ihm J, Zunger A and Cohen M L 1979 *J. Phys. C: Solid State Phys.* **12** 4409
- [57] See *VASP the Guide* <http://cms.mpi.univie.ac.at/VASP/>
- [58] Wu X, Vanderbilt D and Hamann D R 2005 *Phys. Rev. B* **72** 035105
- [59] Fuchs F, Furthmüller J, Bechstedt F, Shishkin M and Kresse G 2007 *Phys. Rev. B* **76** 115109
- [60] Lindefelt U and Zunger A 1982 *Phys. Rev. B* **26** 846
- [61] Anisimov V I, Zaanen J and Andersen O K 1991 *Phys. Rev. B* **44** 943
- [62] Anisimov V I, Solovyev I V, Korotin M A, Czyzyk M T and Sawatzky G A 1993 *Phys. Rev. B* **48** 16929
- [63] Liechtenstein A I, Anisimov V I and Zaanen J 1995 *Phys. Rev. B* **52** R5467
- [64] Dudarev S L, Botton G A, Savrasov S Y, Humphreys C J and Sutton A P 1998 *Phys. Rev. B* **57** 1505
- [65] Pemmaraju C D, Hanafin R, Archer T, Braun H B and Sanvito S 2008 *Phys. Rev. B* **78** 054428
- [66] Perdew J P, Ernzerhof M and Burke K 1996 *J. Chem. Phys.* **105** 9982
- [67] Alkauskas A, Broqvist P, Devynck F and Pasquarello A 2008 *Phys. Rev. Lett.* **101** 106802
- [68] Wang L W and Zunger A 1995 *Phys. Rev. B* **51** 17398
- [69] Wang L W, Franceschetti A and Zunger A 1997 *Phys. Rev. Lett.* **78** 2819
- [70] Blöchl P 1994 *Phys. Rev. B* **50** 17953
- [71] Kresse G and Joubert J 1999 *Phys. Rev. B* **59** 1758
- [72] Bengone O, Alouani M, Hugel J and Blöchl P 2000 *Comput. Mater. Sci.* **17** 146
- [73] Raebiger H, Lany S and Zunger A 2009 *Phys. Rev. B* **79** 165202
- [74] Lany S and Zunger A, unpublished
- [75] Perdew J P, Parr R G, Levy M and Balduz J L 1982 *Phys. Rev. Lett.* **49** 1691
- [76] Perdew J P, Ruzsinszky A, Csonka G I, Vydrov O A, Scuseria G E, Staroverov V N and Tao J 2007 *Phys. Rev. A* **76** 040501
- [77] Mori-Sánchez P, Cohen A J and Yang W 2008 *Phys. Rev. Lett.* **100** 146401
- [78] Coey J M D 2005 *Solid State Sci.* **7** 660
- [79] Droghetti A, Pemmaraju C D and Sanvito S 2008 *Phys. Rev. B* **78** 140404